Identification of Multiple DNA Copy Number Alterations Including Frequent 8p11.22 Amplification in Conjunctival Squamous Cell Carcinoma

Laura Asnaghi,[1] Hind Alkatan,[2] Alka Mahale,[2] Maha Othman,[2] Saeed Alwadani,[1,3,4] Hailah Al-Hussain,[2] Sabah Jastaneiah,[2] Wayne Yu,[5] Azza Maktabi,[2] Deepak P. Edward,[2,3] and Charles G. Eberhart[1,3,6]

[1]Department of Pathology, Johns Hopkins University, School of Medicine, Baltimore, Maryland, United States
[2]King Khaled Eye Specialist Hospital, Riyadh, Saudi Arabia
[3]Department of Ophthalmology, Johns Hopkins University, School of Medicine, Baltimore, Maryland, United States
[4]Department of Ophthalmology, King Saud University, Riyadh, Saudi Arabia
[5]Microarray Core Facility, Sidney Kimmel Cancer Center, Johns Hopkins University, School of Medicine, Baltimore, Maryland, United States
[6]Department of Oncology, Johns Hopkins University, School of Medicine, Baltimore, Maryland, United States

Correspondence: Charles G. Eberhart, Departments of Pathology, Ophthalmology, and Oncology, Johns Hopkins University, School of Medicine, Smith Building, 400 N. Broadway Avenue, Baltimore, MD 21287, USA; ceberha@jhmi.edu.

LA and HA contributed equally to the work presented here and should therefore be regarded as equivalent authors.

Submitted: May 30, 2014
Accepted: November 14, 2014

Citation: Asnaghi L, Alkatan H, Mahale A, et al. Identification of multiple DNA copy number alterations including frequent 8p11.22 amplification in conjunctival squamous cell carcinoma. *Invest Ophthalmol Vis Sci*. 2014;55:8604–8613. DOI:10.1167/iovs.14-14920

Purpose. Little is known about the molecular alterations that drive formation and growth of conjunctival squamous cell carcinoma (cSCC). We therefore sought to identify genetic changes that could be used as diagnostic markers or therapeutic targets.

Methods. The DNA extracted from 10 snap-frozen cSCC tumor specimens and 2 in situ carcinomas was analyzed using array-based comparative genomic hybridization (aCGH), and further examined with NanoString and quantitative PCR.

Results. The number of regions of DNA loss ranged from 1 to 23 per tumor, whereas gains and amplifications ranged from 1 to 15 per tumor. Most large regions of chromosomal gain and loss were confirmed by NanoString karyotype analysis. The commonest alteration was amplification of 8p11.22 in 9 tumors (75%), and quantitative PCR analysis revealed 100-fold or greater overexpression of ADAM3A mRNA from 8p11.22 locus. In addition, recurring losses were observed at 14q13.2 and 22q11.23, both lost in 5 (42%) of the 12 tumors, and at 12p13.31, lost in 4 (33%) of the 12 samples. Of the eight loci associated with the DNA damage repair syndrome xeroderma pigmentosum, three showed loss of at least one allele in our aCGH analysis, including XPA (9q22.33, one tumor), XPE/DDB2 (11p11.2, one tumor) and XPG/ERCC5 (13q33.1, three tumors).

Conclusions. Conjunctival SCC contains a range of chromosomal alterations potentially important in tumor formation and growth. Amplification of 8p11.22 and overexpression of ADAM3A suggests a potential role for this protease. Our findings also suggest that defects in DNA repair loci are important in sporadic cSCC.

Keywords: conjunctiva squamous cell carcinoma (cSCC), array CGH, NanoString assay

A range of precancerous and cancerous epithelial lesions can arise in the cornea and conjunctiva, including actinic keratosis, conjunctival intraepithelial neoplasia (CIN), conjunctival carcinoma in situ (cCIS, sometimes grouped with severe CIN), and conjunctival squamous cell carcinoma (cSCC). Carcinomas arise most commonly in the interpalpebral area, and involve the bulbar conjunctiva and the limbus.[1,2] Although these tumors have a low metastatic potential, they can be locally invasive.[3] Most of the lesions grow slowly and are unilateral. The main reported risk factors for this group of ocular surface squamous neoplasms (OSSN) are high ultraviolet (UV-B) exposure, infection with high-risk subtypes of human papilloma virus (HPV), and suppression of the immune response due to infection with human immunodeficiency virus or medication.[4–6]

The role of HPV in the pathogenesis of cSCC is somewhat controversial. Early investigations detected HPV, but several recent studies have not identified the virus in CIN or cSCC lesions, calling its role in the initiation and growth of these tumors into question.[7–9] The strong association between OSSN and exposure to sunlight, however, is clear, with a striking increase in their incidence in geographic areas that are close to the equator.[4,10,11] In addition, patients with xeroderma pigmentosum, who are more susceptible to the effects of solar UV light due to mutation or loss of DNA repair factors, are especially prone to develop the disease.[12] Despite this evidence supporting a role for mutations and other DNA alterations in OSSN pathogenesis, the genetic drivers responsible for their initiation and progression are largely unknown. We therefore sought to identify chromosomal abnormalities in a series of cSCC and in situ lesions resected at a single center in Saudi Arabia so as to find molecular alterations potentially useful for diagnosis and as targets for therapy.

Table 1. Clinical and Pathological Features of the Ocular Surface Squamous Neoplasia Specimens

Case	Array CGH	NanoString	Age Group	Sex	Size Group	Vascularized	Histopathology	Invasion Outside Conjunctiva	Subsequent Recurrence	Immunosuppression
1	Yes	Yes	3	M	4	Yes	cCIS	Cornea	No	Unknown
2	Yes	Yes	4	M	5	Yes	cSCC	Cornea Orbit	No	No
3	Yes	Yes	4	M	4	Yes	cSCC	Cornea	No	No
4	No	No	4	M	5	No	cSCC	Cornea Sclera Orbit	No	Unknown
5	Yes	Yes	3	F	5	Yes	cSCC	Cornea Orbit	No	No
6	Yes	Yes	4	M	4	Yes	Recurrent cCIS	Cornea	Yes	No
7	Yes	No	3	M	Unknown	Unknown	Unknown	Unknown	No	Unknown
8	Yes	Yes	4	M	4	Yes	cSCC	Cornea	No	No
9	Yes	Yes	3	M	5	Unknown	cSCC	Cornea Orbit	No	No
10	Yes	Yes	3	M	5	Unknown	cSCC with focal adnexal differentiation	Orbit	No	No
11	No	Yes	4	M	5	Yes	Recurrent cSCC	Sclera	Yes	No
12	Yes	Yes	4	M	5	Yes	cSCC	Cornea	Yes	No
13	Yes	Yes	4	M	5	Yes	Poorly differentiated recurrent cSCC	Cornea Sclera Orbit	No	Unknown
14	Yes	Yes	4	M	5	Yes	Recurrent cSCC	Sclera Orbit	Yes	No

Age groups: 3, 45–65 years; 4, >65 years. Size group: 4, 5–10 mm; 5, >10 mm. M, male; F, female; cCIS, conjunctival carcinoma in situ; cSCC, conjunctival squamous cell carcinoma.

Materials and Methods

Clinical Information

In situ and invasive conjunctival squamous cell carcinoma cases were identified through review of pathology and tumor bank records at King Khaled Eye Specialist Hospital (KKESH), Riyadh, Saudi Arabia. Only cases with tissue snap-frozen at the time of surgery were used in this study. The diagnostic slides in all cases were reviewed by ophthalmic pathologists (HA, DE, and AM) to confirm the presence of carcinoma. After Institutional Review Board approval, relevant clinical data were abstracted from the clinical record and linked to the frozen research cases using anonymized sample identification numbers. The clinical characteristics in these cases are summarized in Table 1.

Genomic DNA and Total RNA Extraction

Genomic DNA was extracted from 14 snap-frozen OSSN tumor tissues using DNeasy Blood and Tissue Kit (Qiagen, Germantown, MD, USA) following manufacturer's protocol, and the DNA concentration and quality were determined using a spectrophotometer (NanoDrop Technologies, Wilmington, DE, USA). The DNA in 2 of the 14 samples was not sufficient to perform array comparative genomic hybridization array-based comparative genomic hybridization (aCGH) although one of these was used for NanoString analysis. Total RNA also was isolated from the tumor tissues and additionally from two normal bulbar conjunctiva specimens taken at autopsy using an RNeasy Mini Kit (Qiagen) according to manufacturer's protocol and used for reverse-transcription and quantitative real-time PCR.

Array CGH

The Agilent SurePrint G3 Human 4x 180K Microarray (G4449A) was used in the study (Agilent Technologies, Santa Clara, CA, USA). This array contains 170,334 distinct biological probes chosen from human genome sequences. The integrity of genomic DNA was confirmed by low-voltage 0.6% agarose gel electrophoresis with a mean band size of approximately 50 Kb. Sample labeling was performed following Agilent's recommendation for array CGH. Briefly, 1.5 μg genomic tumor DNA and normal reference DNA were digested with 50 units of Alu I and Rsa I (Promega, Madison, WI, USA) for 2 hours at 37°C. Samples were then purified by using QIAQuick PCR clean-up kit (Qiagen). Labeling reactions were carried out with restricted and purified DNA for 3 hours at 37°C using a BioPrime Array CGH Genomic Labeling Module (Invitrogen, Carlsbad, CA, USA) with 3 μmol Cy5-dUTP or Cy3-dUTP (Perkin Elmer, Waltham, MA, USA). Labeled samples were purified, concentrated on a Centricon YM-30 column (Millipore, Billerica, MA, USA), and then mixed with 10× blocking agent and 2× hybridization buffer (Agilent Technologies). Hybridization mixtures were first denatured at 95°C for 3 minutes and then immediately transferred to 37°C for 30 minutes. To remove any precipitates, the mixtures were centrifuged at 14,000*g* for 5 minutes. These mixtures were then hybridized to the microarrays for 40 hours at 65°C in a rotating oven (Robbins Scientific, Mountain View, CA, USA) at 10 rpm. Hybridized microarrays were washed and dried according to manufacturer's protocols, and imaged with an Agilent G2565BA microarray scanner using default settings. Data were extracted using Feature Extraction Software v9.1 (Agilent Technologies) and analyzed using Agilent's Genome Workbench software (version 7.0). Aberrant regions (gains or losses) were then identified using a build-in Hidden Markov

Investigative Ophthalmology & Visual Science

Models algorithm with default settings. Dye swap experiments were performed for each sample and only aberrations present in both sets were considered for further analysis. The Log_2 [Tumor/Normal] for each probe in a chromosome region was determined and averaged for the region by the algorithm. Values between 0.75 and 1.0 were considered genomic gain, and $\geq$1.0 amplification, whereas those between –0.75 and –1.0 were classified as hemizygous loss, and $\leq$–1.0 as homozygous deletion.

Quantification of Chromosomal Aberrations by NanoString Analysis

For NanoString analysis, 600 ng purified genomic DNA was used from each sample and hybridized overnight in a thermocycler at 65°C with the human karyotype panel probes (NanoString Technologies, Inc., Seattle, WA, USA). Hybridization mixtures were then loaded into the nCounter Prep Station, and color-coded barcodes on the reporter probes were read and quantified by the nCounter Digital Analyzer (NanoString Technologies, Inc.). Copy number estimate for each probe was normalized using a normal DNA reference. Quality control, normalization, and data analysis were performed using nSolver software (NanoString Technologies, Inc.). After normalization, copy number estimate values between 2.5 and 3.0 were scored as genomic gains, greater than 3.0 as high-level amplifications, between 1.0 and 1.5 as hemizygous deletions, and lower than 1.0 as homozygous deletions. Technical variability was reported as being 15%; therefore, we used a conservative threshold of 25%.[13]

Real-Time Quantitative PCR

Expression levels of ADAM3A and ADAM5P transcripts were determined using TaqMan one-step quantitative RT-PCR (Invitrogen), following manufacturer's protocol. Primers specific for ADAM3A (ID: Hs03297297_m1), ADAM5P (ID: Hs01386884_m1), and 18S, used for normalization (ID: Hs99999901_s1), were purchased from Invitrogen. All reactions were performed in triplicate, using 50 ng RNA, in an iQ5 Multicolor real-time PCR detection system (Bio-Rad, Hercules, CA, USA), using EXPRESS One-Step Superscript reverse-transcription and quantitative real-time PCR (qRT-PCR) Kit, universal mix (Invitrogen). The cycling program included the cDNA synthesis at 50°C for 15 minutes, followed by incubation at 95°C for 20 seconds and 40 cycles at 95°C for 3 seconds, and 60°C for 30 seconds, according to manufacturer's protocol.

Results

Clinical Characteristics

The cases with frozen tissue available included 1 primary and 1 recurrent cCIS, as well as 10 primary and 2 recurrent invasive cSCCs resected at KKESH between 2005 and 2010. In some of the recurrent cases, cryotherapy had been used in addition to surgery, but no previous chemotherapy exposure was documented. Five of the patients were between 45 and 65 years of age, with the remainder older than 65; all but one patient were males. Most tumors were well vascularized, and most had invaded into the cornea, sclera, or orbit. None of the patients were known to be immunosuppressed or have a history of HPV infection. Clinical features are summarized in Table 1.

Recurrent DNA Alterations Detected by Array CGH

Array CGH analysis was successful in 12 cases, whereas in two tumors, DNA extracted was insufficient for this testing, as indicated in Table 1. All of the tumors had DNA copy number abnormalities, and a graphical representation of the regions of gain (red) and loss (green) among the entire cohort is shown in Figure 1. In Figure 2, representative data from selected single cases are shown. The changes illustrated include gains in chromosome 2 (p arm, case 8) and chromosome 3 (q arm, case 6). Representative losses in chromosome 2 (terminal part of the q arm, case 8), chromosome 3 (p arm, case 6), chromosome 11 (part of the p-q arms, case 12), and chromosome 13 (q arm, case 6) also are shown. Each tumor sample was analyzed twice using a dye swap protocol, and only alterations identified in both experiments were included in the Tables 2, 3, and Supplementary Tables S1 to S4.

The number of hemizygous or homozygous DNA losses ranged from 1 to 23 per tumor, whereas gains/amplifications ranged from 1 to 15 (Tables 2, 3). These ranged from small changes to entire chromosomal arms. The combined gains and losses varied from 3 to 34 per tumor (mean 15). Case 10, which only had two gains and one loss, was distinct microscopically, with adnexal features. The precise extent of the regions of DNA gain and loss, as well as the amplitude of the changes identified, is summarized in Supplementary Tables S1 and S2.

Large regions of DNA gain or amplification including all of chromosomal arm 3q were identified in three cases, including two cCIS and one cSCC, whereas 5p was gained or amplified in two tumors. Additional large regions of gain or amplification involving either one or both chromosomal arms were noted in only single tumors at chromosome 1q, 8q, 9q, and 20 (Supplementary Table S1). The locus 3q22.3–3q28 was found to be amplified in 4 (33%) of 12 cases, and 2p14–2p25.2 gain was detected in 3 (25%) of 12 cases. Gains in 2 of the 12 tumors were noted at 6p22.1–6p25.2, 6p12.1, or 13q12.12–13q12.3. Finally, the locus 1p31.1 was found to be amplified in three cases and lost in two. Among the regions smaller than 1 Mb of increased DNA copy number, the commonest recurring alteration was identified at 8p11.22, which was amplified in 9 (75%) of 12 cases. We also examined two frozen normal bulbar conjunctival specimens from adult autopsy patients, and did not identify any large regions of gain or loss. No amplification of 8p11.22 was noted in either of these healthy controls, but low-level DNA gains were found at this locus.

Large recurring regions of loss, encompassing one entire chromosome arm, included 3p, 4p, 13q, 14q, and 17p, with additional large regions lost in only single tumors (Supplementary Table S2). More focal regions of DNA loss greater than 1 Mb in size were present in more than one case at 4q34.3–4q35.2, 5q11.1–5q14.3, 8p21.2–8p23.2, 9p13.2–9p24.2, 11p15.2–11p15.4, 12p13.2–12p13.32, and 18q12.3–18q22.3. Recurring small losses (less than 1 Mb) were located at 14q13.2 and 22q11.23, which were both lost in 5 (42%) of the 12 samples, 12p13.31, lost in 4 (33%) of the 12 samples, and 8p11.22 lost in 3 (25%) of the 12 samples. None of these focal DNA losses were found in the normal bulbar conjunctival specimens. The most common recurrent homozygous deletions greater than 1 Mb included the loci 11p15.4, most of the short arm of chromosome 17, and most of the long arm of chromosome 13, all of which were found to be deleted in 3 (25%) of 12 samples, as shown in Supplementary Table S2.

Interestingly, one of the DNA repair genes associated with xeroderma pigmentosum, a condition that predisposes patients to cSCC, is located within the region of loss on chromosome 13q. The 13q33.1 locus encoding XPG/ERCC5 was lost in cases 6, 8, and 9. Two other xeroderma pigmentosum genes were also found to be lost in single cases: the XPA gene at 9q22.33 (case 8) and the XPE/DDB2 gene at 11p11.2 (case 14).

Investigative Ophthalmology & Visual Science

Figure 1. Graphic representation of all chromosomal changes. The regions of DNA gain (*red*) and loss (*green*) among the entire cohort are shown, with the magnitude of the change representing the number of cases with alterations in each region.

Investigative Ophthalmology & Visual Science

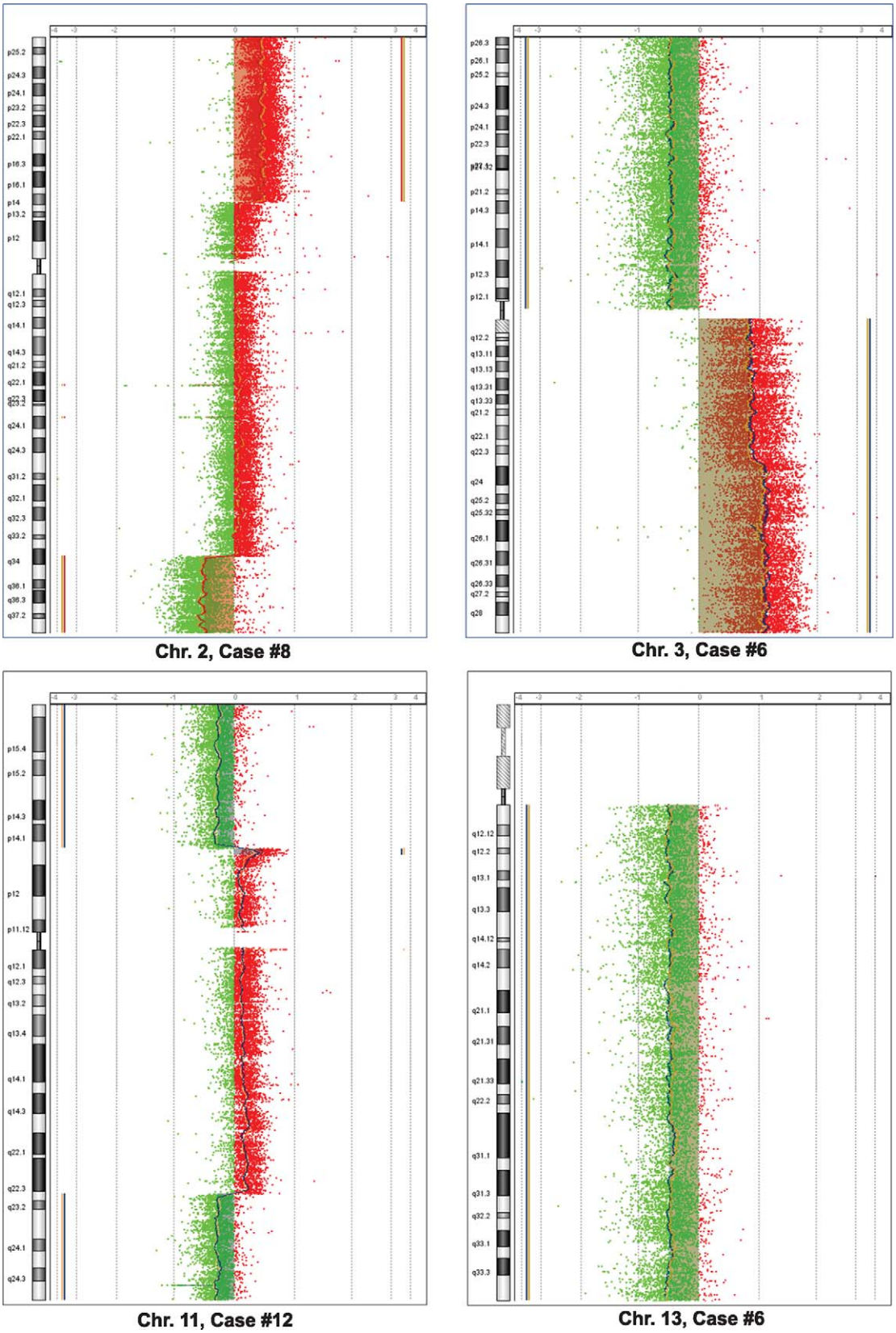

Figure 2. Chromosomal alterations in selected single cases. Each *dot* corresponds to a single probe, with deflections to the *left* of the "0" midline representing reduced hybridization ratio of tumor DNA to that probe, and deflections to the *right* representing an increased hybridization ratio of tumor DNA to that probe. These correspond to loss and gain of DNA at the respective chromosomal loci. Log_2 [Tumor/Normal] for each probe in a chromosome region was determined and values between 0.75 and 1.0 were considered genomic gain, $\geq$1.0 amplification, between −0.75 and −1.0 hemizygous loss, and ≤ -1.0 homozygous deletion. The thin pairs of lines to the *left* or *right* of each alteration indicate that such loss or gain was identified in both of the paired analyses that were performed for each DNA sample according to the dye swap protocol.

Investigative Ophthalmology & Visual Science

Table 2. Chromosomal Gains Detected in the Ocular Surface Squamous Neoplasia Samples

Case No.	Genomic Gains	No. Alterations
1	5p; 7q11.22; 22q11.23 **3q**	4
2	1p31.1; 12p13.31; 20q13.33; **8p11.22**	4
3	3q; 6p12.1 **8p11.22**	3
5	16p11.2	1
6	9q; 16p12.3–16p13.2; 18p11.31 **1q; 3q; 8p11.22; 9p21.3**	7
7	7p14.1–7p22.2; 12p13.31 **8p11.22**	3
8	2p14–2p25.2; 6p22.1–6p25.2; 8p21.3; 19q13.41–19q13.43; 20 **6q22.31–6q27; 13q12.12–13q12.3; 13q14.11**	8
9	2p14–2p25.2; 16p11.2; 19q13.2–19q13.31 **8p11.22**	4
10	1p31.1 **8p11.22**	2
12	1p12–1p35.1; 2p14–2p25.2; 3q22.3–3q28; 7p22.2; 9p24.2; 10p12.33–10p15.2; 12p13.31; 16q22.2–16q23.3; 20q13.13–20q13.33; 22q11.23; **6p12.1–6p21.2; 6p24.3–6p25.2; 8p11.22; 13q12.12–13 q12.3; 17q12**	15
13	8q; 14q21.3 **5p; 8p11.22**	4
14	6p22.1–6p25.2; 11p12–11p15.1; 17q22–17q25.2 **8p11.22; 11p11.2–11p12**	5

Amplifications (amplitude ≥ 1) are shown in bold.

Table 3. Chromosomal Losses Detected in the Ocular Surface Squamous Neoplasia Samples

Case No.	Genomic Losses	No. Alterations
1	1q21.2; 2p23.1; 2q22.1; 9p23–9p24.1; 11q11; 14q13.2–14q21.3; 14q23.3; 15q11.2–15q13.1; 18q12.2–18q12.3; 21q21.1; **1p31.1; 8p11.22; 11p15.4; 20p12.1; 22q12.3**	15
2	1q21.2; 10q11.22; **3p22.3; 7p12.1; 11q11**	5
3	**2p22.1; 22q11.23**	2
5	3p21.2; 5q13.2; 5q23.2; 7q11.23; 7q22.3; 10q21.3; 10q24.32; 12q13.3; 12q24.31; 12q23.3–12q24.1; 14q13.2; 15q21.2; 15q22.31; 16p13.12; 16q22.2; 17q21.31; 17q22; 22q12.2; **3q21.2; 3q26.1; 6p22.1; 8p11.22; 22q11.23**	23
6	4p; 4q31.21–4q34.3; 6p11.2; 17p; **3p; 6p21.32; 8p21.2–8p23.2; 13q; 22q11.23**	9
7	14q; 18q12.3–18q22.3; **1q31.3; 7p12.1; 11q11**	5
8	2q22.1; 2q24.2; 3p24.3; 9p13.2–9p24.2; 18q12.3–18q22.3; **2q34–2q37.2; 3q26.1; 7p; 7q31.1–7q36.2; 8p11.22; 9q; 10p; 11p15.2–11p15.4;** **12p13.2–12p13.32; 13q14.12–13q33.3; 14q12–14q21.1; 17p12; 22q**	18
9	1q21.2; 4p; 6p22.1; 9p13.2–9p24.2; 13q; 14q; 17p; 19q13.33; **1p31.1; 3p; 6p21.32**	11
10	12p13.31	1
12	4q34.3–4q35.2; 4q22.1; 5q11.1–5q14.3; 6p22.3; 7p12.1–7p15.2; 9p21.3; 10q11.22; 10q22.2; 10q23.31–10q26.2; 11p13–11p15.4; 11q23.2–11q24.3; 16p12.1–16q12.3; 16q12.2; 18; 20p12.1–20p12.3; 21q22.2; 21q21.2–21q22.11; **8p21.2–8p23.2; 14q21.1**	19
13	9p21.3; 17q21.31; 19p13.11–19p12; 12p13.31; **22q12.3**	5
14	5q; 9p13.2–9p24.2; 11p11.12–11p12; 12p; **6p21.32**; **11p15.2–11p15.4; 22q11.23**	7

Homozygous deletions are shown in bold (amplitude ≤ -1).

Confirmation of Gains and Losses

We used the NanoString platform to confirm chromosomal alterations identified by array-based comparative genomic hybridization (aCGH; Fig. 3). A total of 338 probes were included in the NanoString karyotype panel, in addition to control probes targeting invariant genomic regions used for normalization. The much lower density of probes as compared with array CGH meant that only very large regions of gain or loss could be identified using this technique. Among larger regions of gain identified by array CGH, 14 (54%) of 26 were confirmed by all corresponding NanoString probes (complete confirmation), 9 (34.5%) of 26 were confirmed by some but not all of the corresponding probes (partial confirmation), and 3 (11.5%) were not confirmed. For the large deletions, 12 (34.3%) of 35 were completely confirmed, 19 (54.3%) of 35 were partially confirmed, and 4 (11.4%) were not confirmed, as shown in Figure 3 and Supplementary Table S3.

Representative NanoString analysis for loci on chromosome 3 is shown in Figure 3. We found by array CGH gain of almost the entire 3q arm in samples 1, 3, and 6, whereas a somewhat smaller region encompassing more than half of the arm (3q22.3–3q28) was amplified in sample 12 (Fig. 3, center). According to the NanoString analysis, all probes on the 3q arm were gained in samples 1 and 6 (complete confirmation), whereas half of the relevant probes showed significant gains (copy number estimate values greater than 2.5) in sample 3 (partial confirmation). All of the relevant probes within the smaller region of gain identified in case 12 also were confirmed using the NanoString platform (Fig. 3, bottom). No NanoString probes were located in proximity to the recurring gain that we identified by array CGH at 8p11.22, thus we had to further analyze this locus using other methods.

Analysis of 8p11.22 Locus

The most frequent genomic alteration was observed on chromosome 8 (Fig. 4A), where the locus 8p11.22 was amplified in 9 (75%) of 12 tumors. Interestingly in the other three cases this locus appeared to be at least partially lost. The region contains a group of genes coding for "a disintegrin and metalloprotease" (ADAM) proteins, which are peptidases involved in the shedding and activation of oncogenic receptors, in tumor formation and cell migration. In particular, the locus includes the *ADAM1B*, *ADAM3A*, and *ADAM5P* genes (Fig. 4A, right). Upregulation of the

AMPLIFICATIONS >1Mb
Total = 26
14 confirmed (54%)
9 partially confirmed (34.5%)
3 not confirmed (11.5%)

DELETIONS >1Mb
Total = 35
12 confirmed (34.3%)
19 partially confirmed (54.3%)
4 not confirmed (11.4%)

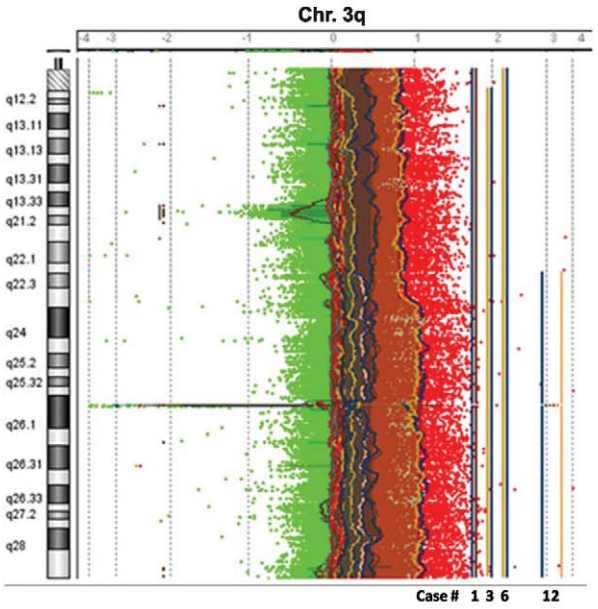

Copy Number Estimate	1	2	3	5	6	8	9	10	11	12	13	14
3q13.11	3.3	2.05	2.54	1.28	3.92	2.16	2.24	2.24	1.84	2.15	2.33	2.05
3q13.32	3.09	2.2	2.28	2.5	3.91	2.35	2.02	2.14	2.07	2.07	2.32	2.12
3q21.3	2.87	1.69	2.09	1.65	3.61	1.45	1.83	1.83	1.67	2.03	1.95	1.7
3q23	3.76	2.2	2.65	2.32	4.11	2.55	2.42	2.42	2.11	3.14	2.47	2.44
3q25.2	3.24	2.44	2.77	2.22	5.15	2.47	2.39	2.58	2.3	2.98	2.44	2.14
3q26.1	2.59	2.23	2.55	2.44	4.5	2.14	2.42	2.33	1.82	2.84	2.43	2.33
3q26.32	2.66	1.96	2.24	3.02	4.11	1.04	1.95	1.91	1.76	2.65	2.18	1.94
3q28	2.62	2.01	2.23	2.05	3.91	1.85	2.19	1.93	1.81	2.75	2.08	2.03

: gain

Copy Number Estimate = 2.5 - 3.0 genomic gain
> 3.0 high-level amplification
= 1.0 - 1.5 hemizygous deletion
< 1.0 homozygous deletion

Figure 3. Confirmation of chromosomal changes using NanoString. Comparison between the copy number variation (CNV) alterations identified by array CGH and NanoString platform shows that among the larger regions of DNA gain identified by aCGH, 14 (54%) of 26 were confirmed by all corresponding NanoString probes (complete confirmation), 9 (34.5%) of 26 were confirmed by some but not all of the corresponding probes (partial confirmation) and 3 (11.5%) were not confirmed. For the large deletions, 12 (34.3%) of 35 were completely confirmed, 19 (54.3%) of 35 were partially confirmed, and 4 (11.4%) were not confirmed. After normalization, NanoString copy number estimate values between 2.5 and 3.0 were scored as genomic gains, greater than 3.0 as high-level amplifications, between 1.0 and 1.5 as hemizygous deletions, and lower than 1.0 as homozygous deletions.

ADAM3A locus was confirmed at the RNA level by TaqMan one-step quantitative RT-PCR, normalized to 18S mRNA levels (Fig. 4B). Normal bulbar conjunctival tissue from two eyes was used as an additional control. We observed that the ADAM3A gene was at least 100 times more highly expressed in five of the nine samples (cases 2, 3, 7, 12, and 13) where we detected high-level amplification by aCGH, as compared with cases 1 and 5, which showed genomic loss in this locus by aCGH. There was insufficient RNA to analyze samples 6, 8, 9, and 10 by real-time PCR. These five tumors with DNA amplification at the locus 8p11.22 also showed mRNA levels of ADAM3A approximately 100 times higher than non-neoplastic conjunctiva. One tumor (case 14) was found to have amplification of 8p11.22 by aCGH, but did not show increased expression of ADAM3A. Quantitative RT-PCR was also performed to determine the expression of ADAM5P gene, which maps in a region partially included in the 8p11.22 region of gain. However, in contrast to ADAM3A, ADAM5P mRNA was not detected in the tumor samples (data not shown).

Investigative Ophthalmology & Visual Science

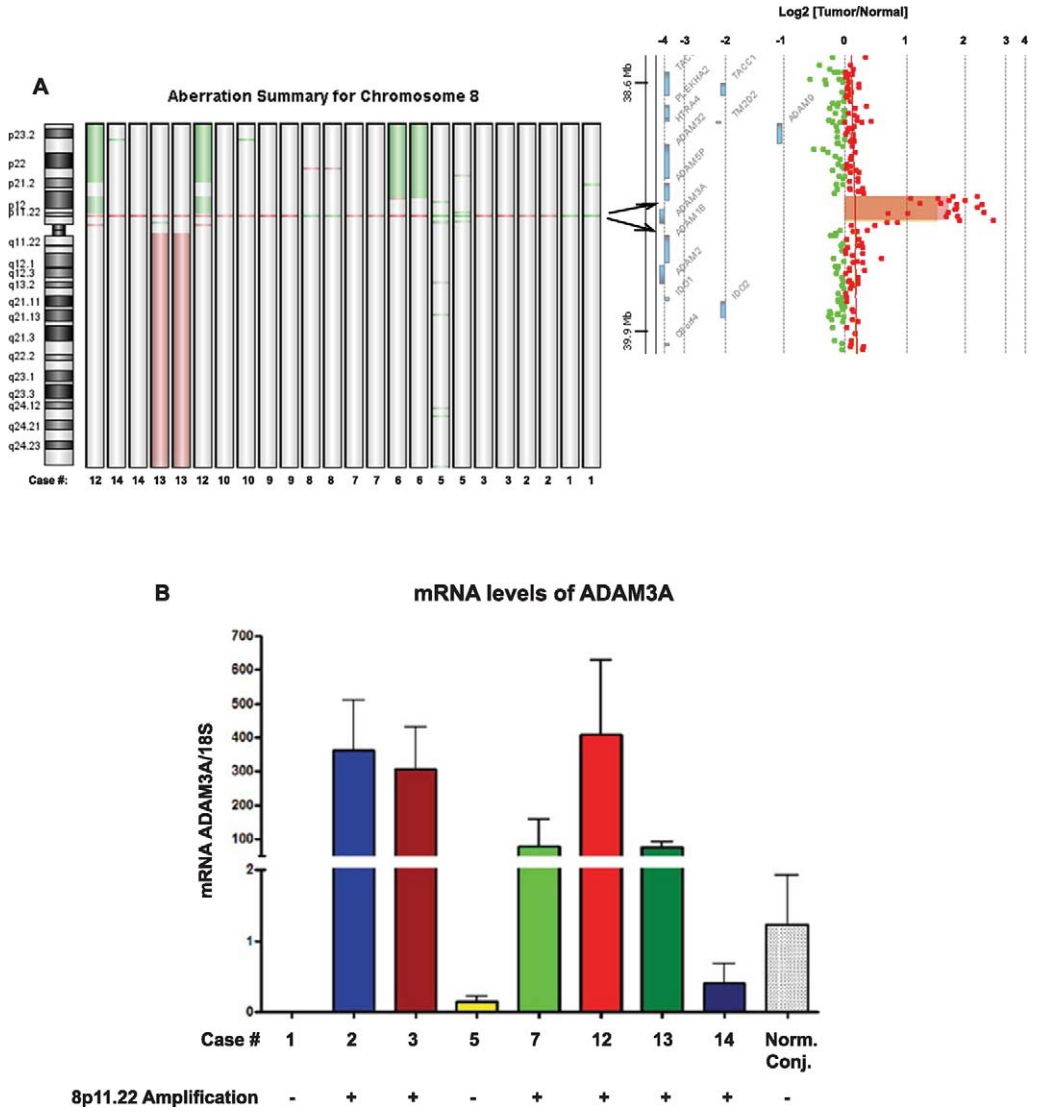

Figure 4. Expression of mRNA at the 8p11.22 locus. The most frequent DNA amplification was detected at 8p11.22. (**A**) Genomic aberration summary of chromosome 8 is shown for all the samples analyzed, with dye swap performed for each of them. *Green* indicates regions of loss and *red* regions of gain. The heat map shows DNA gain in the locus 8p11.22 in 9 of the 12 samples. The gene view on the *right* shows that such amplification involves ADAM3A and part of the ADAM5P genes. (**B**) Upregulation of ADAM3A as compared with non-neoplastic conjunctiva was confirmed in cases 2, 3, 7, 12, and 13 at the RNA level using TaqMan one-step quantitative RT-PCR normalized to 18S mRNA. Normal bulbar conjunctival tissue was used as internal control. For cases 6, 8, 9, and 10, there was not enough RNA to perform the real-time PCR.

Discussion

Ocular surface squamous neoplasms are most common in countries near the equator with increased exposure to sunlight, suggesting a role for DNA damage due to UV exposure.[14,15] The incidence in the United States is 0.03 cases per 100,000 persons, whereas in Australia it is 1.9 cases per 100,000 persons.[16] Conjunctival SCC also is common in Saudi Arabia, with one report noting that most patients spent significant time outdoors, and that advanced cases requiring orbital exenteration were common.[17] A more recent study reviewing the KKESH tumor registry over the past three decades found that cSCC incidence has remained steady, and that it still represents the most common ocular malignancy diagnosed in adults at this tertiary eye hospital.[18]

Using aCGH, we identified a number of recurring chromosomal aberrations in the analysis of 10 cSCC and 2 cCIS specimens. To our knowledge, no detailed chromosomal analyses of OSSN have been published, thus we are not able to compare these results to previous studies. However, we found that in 4 of the 12 tumor samples there was loss of one or more loci containing three of the eight genes responsible for the repair of the UV-induced DNA defects and altered in xeroderma pigmentosum. To the best of our knowledge, the genes *XPA*, *XPE/DDB2*, and *XPG/ERCC5* have not been previously examined in sporadic cSCC, and their loss suggests DNA repair defects also may contribute to tumor formation or progression in nonsyndromic cases.

Less direct evidence implicating changes to DNA repair also were identified. At chromosome 22q11.23, five tumors showed DNA loss and two DNA gain. Deletions of 22q11.23 have previously been reported in cervical SCC, chronic lymphocytic leukemia, and ovarian adenocarcinoma.[19–21] Interestingly, this locus contains several genes involved in glutathione metabolism, including Glutathione S-Transferase τ, whose deletion has been found in ovarian, cervical, and endometrial carcinoma

cells.[22,23] Such deletion has been reported to predispose to mutations in the p53 gene in breast cancer.[24] Alterations in p53 expression have also been detected in OSSN, and p53 is known to play a crucial role in the nucleotide excision repair, a pathway for repair of UV-induced DNA damage.[25,26] Thus, these changes may relate to the defects in xeroderma pigmentosum genes described above.

A number of other regions of gain and loss we identified have been implicated in the pathogenesis of other tumor types. For example, chromosome 6p21.32 was lost in 3 of 12 of our cases. Deletions including this region also have been reported in nasopharyngeal carcinoma.[27,28] Chromosome 14q13.2 was lost in 4 (33%) of the 12 OSSN samples, and this region contains a number of genes, including PAX9 and FOXG1, that play key roles in normal development and carcinogenesis.[29] The locus 12p13.31 was deleted in 4 of the 12 samples and gained in 3. Interestingly, the region 12p13 has been found to be genetically unstable and fragile in patients with lymphoid and myeloid hematologic malignancies.[30] We also found that the locus 1p31.1 was lost in two samples and gained in another three. High levels of loss of heterozygosity were found in 1p31 locus, along with other regions in the p arm of chromosome 1, in different human solid tumors.[31]

We also examined if any DNA changes in our cases could be linked to cutaneous SCC or HPV-associated cervical and oropharyngeal carcinomas, and a summary of relevant recurring chromosomal abnormalities is shown in Supplementary Table S4.[32–42] Similarities include DNA gains that we observed in 3q22.3–3q28 and in 5p, as well as DNA losses in 9p, 13q, 17p, and 18q, which also are found in cutaneous SCC.[34] A smaller number of changes, which were similar in our tumors and HPV-associated neoplasms outside the eye are also listed in Supplementary Table S4.

Our study was too small to tightly link clinical features with genetic changes. However, one of the four recurrent tumors, case 12, had the highest number of DNA gains (15) and the second highest number of DNA losses (19), thus an increased number of DNA alterations in some cases may be associated with more aggressive clinical behavior or tumor progression. Larger studies that include cases drawn from other ethnic groups and geographical regions will need to be performed to address this issue, as well as to confirm our genetic observations in this single-institution cohort.

The most frequent chromosomal variation was observed on chromosome 8, where 8p11.22 was amplified in nine tumors (75%). This region contains a group of genes coding for ADAM proteins known to be involved in the activation of oncogenic receptors and tumor formation and spread.[43] The ADAMs are transmembrane proteins that contain a disintegrin and a metalloprotease domain, and have both cell adhesion and protease activities. Their functions include activation of membrane receptors (Notch and HER2), cell migration, and cytokine and growth factor shedding.[44–47] The *ADAM* gene family includes 29 members, but the function of most of the *ADAM* gene products is still unknown.

The amplicon that we found includes parts of the ADAM1B, ADAM3A, and ADAM5P loci (Fig. 4A), and is near to the ADAM9 locus recently found to be commonly amplified in oral mucosal SCC.[48] Using TaqMan RT-PCR, we confirmed an approximately 100-fold or greater increased expression from the ADAM3A locus in amplified cases as compared with deleted ones or normal conjunctiva. We did not detect expression of ADAM5P in the tumors. Interestingly, 8p11.22 was lost in the three cases without amplification of the locus. Homozygous loss of *ADAM3A* locus has been reported in pediatric high-grade glioma, but the biological function of the deletion in this tumor type has not been identified.[49] It is not clear why this locus would be either lost or amplified in all cases examined.

In summary, we found frequent DNA copy number alterations in cSCC samples, including gains and losses of large DNA regions and more focal changes encompassing a limited number of loci. The most frequent focal homozygous loss was found in 22q11.23, whose deletion predisposes to p53 mutation in breast cancer. Loss of loci encoding three genes altered in xeroderma pigmentosum also was found in four cases. The predominant amplification was observed at the 8p11.22 locus, where ADAM3A is located, and this family of genes has recently been implicated in mucous membrane carcinomas. Our studies thus confirm the importance of DNA repair in cSCC, and suggest that ADAM proteases might also play a role.

Acknowledgments

Supported by King Khaled Eye Specialist Hospital–Wilmer Eye Institute Collaborative Research Grant and by Research to Prevent Blindness Wilmer Eye Institute. Sample quality assessment and array CGH analysis were conducted at The Sidney Kimmel Cancer Center Microarray Core Facility at the Johns Hopkins University, supported by National Institutes of Health Grant P30 CA006973 entitled Regional Oncology Research Center.

Disclosure: **L. Asnaghi**, None; **H. Alkatan**, None; **A. Mahale**, None; **M. Othman**, None; **S. Alwadani**, None; **H. Al-Hussain**, None; **S. Jastaneiah**, None; **W. Yu**, None; **A. Maktabi**, None; **D.P. Edward**, None; **C.G. Eberhart**, None

References

1. Grossniklaus HE, Green WR, Luckenbach M, Chan CC. Conjunctival lesions in adults. A clinical and histopathologic review. *Cornea*. 1987;6:78–116.
2. Kiire CA, Srinivasan S, Karp CL. Ocular surface squamous neoplasia. *Int Ophthalmol Clin*. 2010;50:35–46.
3. Shields JA, Shields CL, Gunduz K, Eagle RC Jr. The 1998 Pan American Lecture. Intraocular invasion of conjunctival squamous cell carcinoma in five patients. *Ophthal Plast Reconstr Surg*. 1999;15:153–160.
4. Lee GA, Hirst LW. Ocular surface squamous neoplasia. *Surv Ophthalmol*. 1995;39:429–450.
5. Alam M, Ratner D. Cutaneous squamous-cell carcinoma. *N Engl J Med*. 2001;344:975–978.
6. Shields CL, Ramasubramanian A, Mellen PL, Shields JA. Conjunctival squamous cell carcinoma arising in immunosuppressed patients (organ transplant, human immunodeficiency virus infection). *Ophthalmology*. 2011;118:2133–2137.
7. Basti S, Macsai MS. Ocular surface squamous neoplasia: a review. *Cornea*. 2003;22:687–704.
8. Ateenyi-Agaba C, Franceschi S, Wabwire-Mangen F, et al. Human papillomavirus infection and squamous cell carcinoma of the conjunctiva. *Br J Cancer*. 2010;102:262–267.
9. Peralta R, Valdivia A, Estañol P, et al. Low frequency of human papillomavirus infection in conjunctival squamous cell carcinoma of Mexican patients. *Infect Agent Cancer*. 2011;6:24.
10. Newton R, Ferlay J, Reeves G, Beral V, Parkin DM. Effect of ambient solar ultraviolet radiation on incidence of squamous-cell carcinoma of the eye. *Lancet*. 1996;347:1450–1451.
11. Pe'er J. Ocular surface squamous neoplasia. *Ophthalmol Clin North Am*. 2005;18:1–13.
12. Gupta N, Sachdev R, Tandon R. Ocular surface squamous neoplasia in xeroderma pigmentosum: clinical spectrum and outcome. *Graefes Arch Clin Exp Ophthalmol*. 2011;249:1217–1221.
13. Geiss GK, Bumgarner RE, Birditt B, et al. Direct multiplexed measurement of gene expression with color-coded probe pairs. *Nat Biotechnol*. 2008;26:317–325.

14. Sun EC, Fears TR, Goedert JJ. Epidemiology of squamous cell conjunctival cancer. *Cancer Epidemiol Biomarkers Prev*. 1997;6:73–77.
15. Mittal R, Rath S, Vemuganti GK. Ocular surface squamous neoplasia. Review of etio-pathogenesis and an update on clinico-pathological diagnosis. *Saudi J Ophthalmol*. 2013;27:177–186.
16. Lee GA, Hirst LW. Incidence of ocular surface epithelial dysplasia in metropolitan Brisbane. A 10-year survey. *Arch Ophthalmol*. 1992;119:525–527.
17. Huaman A, Cavender JC. Tumors of the eye in Saudi Arabia. *Ann Saudi Med*. 1991;11:675–680.
18. Khandekar RB, Al-Towerki AA, Al-Katan H, et al. Ocular malignant tumors. Review of the Tumor Registry at a tertiary eye hospital in central Saudi Arabia. *Saudi Med J*. 2014;35:377–384.
19. Choi YW, Bae SM, Kim YW, et al. Gene expression profiles in squamous cell cervical carcinoma using array-based comparative genomic hybridization analysis. *Int J Gynecol Cancer*. 2007;17:687–696.
20. Tyybakinoja A, Vilpo J, Knuutila S. High-resolution oligonucleotide array-CGH pinpoints genes involved in cryptic losses in chronic lymphocytic leukemia. *Cytogenet Genome Res*. 2007;118:8–12.
21. Sung CO, Choi CH, Ko YH, et al. Integrative analysis of copy number alteration and gene expression profiling in ovarian clear cell adenocarcinoma. *Cancer Genet*. 2013;206:145–153.
22. Howells RE, Holland T, Dhar KK, et al. Glutathione S-transferase GSTM1 and GSTT1 genotypes in ovarian cancer: association with p53 expression and survival. *Int J Gynecol Cancer*. 2001;11:107–112.
23. Ueda M, Hung YC, Terai Y, et al. Glutathione S-transferase GSTM1, GSTT1 and p53 codon 72 polymorphisms in human tumor cells. *Hum Cell*. 2003;16:241–251.
24. Gudmundsdottir K, Tryggvadottir L, Eyfjord JE. GSTM1, GSTT1, and GSTP1 genotypes in relation to breast cancer risk and frequency of mutations in the p53 gene. *Cancer Epidemiol Biomarkers Prev*. 2001;10:1169–1173.
25. Mahomed A, Chetty R. Human immunodeficiency virus infection, Bcl-2, p53 protein, and Ki-67 analysis in ocular surface squamous neoplasia. *Arch Ophthalmol*. 2002;120:554–558.
26. Smith ML, Ford JM, Hollander MC, et al. p53-mediated DNA repair responses to UV radiation: studies of mouse cells lacking p53, p21, and/or gadd45 genes. *Mol Cell Biol*. 2000;20:3705–3714.
27. Tse KP, Su WH, Yang ML, et al. A gender-specific association of CNV at 6p21.3 with NPC susceptibility. *Hum Mol Genet*. 2011;20:2889–2896.
28. Tsao SW, Yip YL, Tsang CM, et al. Etiological factors of nasopharyngeal carcinoma. *Oral Oncol*. 2014;50:330–338.
29. Santen GW, Sun Y, Gijsbers AC, et al. Further delineation of the phenotype of chromosome 14q13 deletions: (positional) involvement of FOXG1 appears the main determinant of phenotype severity, with no evidence for a holoprosencephaly locus. *J Med Genet*. 2012;49:366–372.
30. Sato Y, Kobayashi H, Suto Y, et al. Chromosomal instability in chromosome band 12p13: multiple breaks leading to complex rearrangements including cytogenetically undetectable subclones. *Leukemia*. 2001;15:1193–1202.
31. Ragnarsson G, Eiriksdottir G, Johannsdottir JT, Jonasson JG, Egilsson V, Ingvarsson S. Loss of heterozygosity at chromosome 1p in different solid human tumours: association with survival. *Br J Cancer*. 1999;79:1468–1474.
32. Son JW, Jeong KJ, Jean WS, et al. Genome-wide combination profiling of DNA copy number and methylation for deciphering biomarkers in non-small cell lung cancer patients. *Cancer Lett*. 2011;311:29–37.
33. Lin M, Smith LT, Smiraglia DJ, et al. DNA copy number gains in head and neck squamous cell carcinoma. *Oncogene*. 2006;25:1424–1433.
34. Ashton KJ, Weinstein SR, Maguire DJ, Griffiths LR. Chromosomal aberrations in squamous cell carcinoma and solar keratoses revealed by comparative genomic hybridization. *Arch Dermatol*. 2003;139:876–882.
35. Salgado R, Toll A, Alameda F, et al. CKS1B amplification is a frequent event in cutaneous squamous cell carcinoma with aggressive clinical behaviour. *Genes Chromosomes Cancer*. 2010;49:1054–1061.
36. Hu Z, Wu C, Shi Y, et al. A genome-wide association study identifies two new lung cancer susceptibility loci at 13q12.12 and 22q12.2 in Han Chinese. *Nat Genet*. 2011;43:792–796.
37. Kalantari M, Blennow E, Hagmar B, Johansson B. Physical state of HPV16 and chromosomal mapping of the integrated form in cervical carcinomas. *Diagn Mol Pathol*. 2001;10:46–54.
38. Schmitz M, Driesch C, Jansen L, Runnebaum IB, Dürst M. Non-random integration of the HPV genome in cervical cancer. *PLoS One*. 2012;7:e39632.
39. Choi YW, Bae SM, Kim YW, et al. Gene expression profiles in squamous cell cervical carcinoma using array-based comparative genomic hybridization analysis. *Int J Gynecol Cancer*. 2007;17:687–696.
40. Coon SW, Savera AT, Zarbo RJ, et al. Prognostic implications of loss of heterozygosity at 8p21 and 9p21 in head and neck squamous cell carcinoma. *Int J Cancer*. 2004;111:206–212.
41. Lehmann AR, McGibbon D, Stefanini M. Xeroderma pigmentosum. *Orphanet J Rare Dis*. 2011;6:70.
42. Jung AC, Briolat J, Millon R, et al. Biological and clinical relevance of transcriptionally active human papillomavirus (HPV) infection in oropharynx squamous cell carcinoma. *Int J Cancer*. 2010;126:1882–1894.
43. Edwards DR, Handsley MM, Pennington CJ. The ADAM metalloproteinases. *Mol Aspects Med*. 2008;29:258–289.
44. Black RA, White JM. ADAMs: focus on the protease domain. *Curr Opin Cell Biol*. 1998;10:654–659.
45. Brou C, Logeat F, Gupta N, et al. A novel proteolytic cleavage involved in Notch signaling: the role of the disintegrin-metalloprotease TACE. *Mol Cell*. 2000;5:207–216.
46. Liu PC, Liu X, Li Y, et al. Identification of ADAM10 as a major source of HER2 ectodomain sheddase activity in HER2 overexpressing breast cancer cells. *Cancer Biol Ther*. 2006;5:657–664.
47. Schwarz J, Schmidt S, Will O, et al. Polo-like kinase 2, a novel ADAM17 signaling component, regulates tumor necrosis factor α ectodomain shedding. *J Biol Chem*. 2014;289:3080–3093.
48. Vincent-Chong VK, Anwar A, Karen-Ng LP, et al. Genome wide analysis of chromosomal alterations in oral squamous cell carcinomas revealed over expression of MGAM and ADAM9. *PLoS One*. 2013;8:e54705.
49. Barrow J, Adamowicz-Brice M, Cartmill M, et al. Homozygous loss of ADAM3A revealed by genome-wide analysis of pediatric high-grade glioma and diffuse intrinsic pontine gliomas. *Neuro Oncol*. 2011;13:212–222.

Investigative Ophthalmology & Visual Science